

# Evidence for dark matter in the inner Milky Way

Fabio Iocco<sup>1,2\*</sup>, Miguel Pato<sup>3,4</sup> and Gianfranco Bertone<sup>5</sup>

**The ubiquitous presence of dark matter in the Universe is today a central tenet in modern cosmology and astrophysics<sup>1</sup>. Throughout the Universe, the evidence for dark matter is compelling in dwarfs, spiral galaxies, galaxy clusters as well as at cosmological scales. However, it has been historically difficult to pin down the dark matter contribution to the total mass density in the Milky Way, particularly in the innermost regions of the Galaxy and in the solar neighbourhood<sup>2</sup>. Here we present an up-to-date compilation of Milky Way rotation curve measurements<sup>3–13</sup>, and compare it with state-of-the-art baryonic mass distribution models<sup>14–26</sup>. We show that current data strongly disfavour baryons as the sole contribution to the Galactic mass budget, even inside the solar circle. Our findings demonstrate the existence of dark matter in the inner Galaxy without making any assumptions about its distribution. We anticipate that this result will compel new model-independent constraints on the dark matter local density and profile, thus reducing uncertainties on direct and indirect dark matter searches, and will help reveal the structure and evolution of the Galaxy.**

Existing studies of the dark matter density in the inner Galaxy fall into two categories: mass modelling and local measurements. In mass modelling, the distribution of dark matter is assumed to follow a density profile inspired by numerical simulations, typically an analytic fit such as the well-known Navarro–Frenk–White<sup>27</sup> or Einasto<sup>28</sup> profiles, with two or more free parameters whose best-fit values are then determined from dynamical constraints. The statistical error on the dark matter density in the inner Galaxy—and in particular in the solar neighbourhood—is in this case very small<sup>29</sup>, of the order of 10%, but this reflects only the strong assumptions made about the distribution of dark matter. The dark matter density profile is in fact observationally unknown, and the aforementioned classes of profiles are inspired by simulations without baryons, whose role is not negligible in the inner Galaxy. Local measurements are instead based on the study of observables in the solar neighbourhood<sup>2</sup>. These methods can be used to assess the evidence for dark matter locally through an estimate of the gravitational potential from the kinematics of stars. However, the value found for the local dark matter density is usually compatible with zero at  $\sim 3\sigma$  unless one makes strong assumptions about the dynamics of the tracer populations.

Here we report on a comparison of the observed rotation curve of the Galaxy with that expected from visible matter alone. As we shall see, this approach provides an alternative way to constrain additional contributions of matter to the rotation curve, and therefore to infer the existence and abundance of dark matter. Although this has been historically one of the first methods to detect dark matter in external galaxies, it has long been thought to provide

weak constraints in the innermost regions of the Milky Way, due to a combination of poor rotation curve data and large uncertainties associated with the distribution of baryons. We show that recent improvements on both fronts allow us to obtain a convincing proof of the existence of dark matter inside the solar circle.

We start by presenting a new, comprehensive compilation of rotation curve data derived from kinematic tracers of the Galactic potential, which considerably improves on earlier (partial) compilations<sup>30,31</sup>. Optimized to Galactocentric radii  $R = 3\text{--}20$  kpc, our database includes gas kinematics (HI terminal velocities<sup>3,4</sup>, CO terminal velocities<sup>5</sup>, HI thickness<sup>6</sup>, HII regions<sup>7,8</sup>, giant molecular clouds<sup>8</sup>), star kinematics (open clusters<sup>9</sup>, planetary nebulae<sup>10</sup>, classical cepheids<sup>11</sup>, carbon stars<sup>12</sup>) and masers<sup>13</sup>. This represents an exhaustive survey of the literature that intentionally excludes objects with only kinematic distances, and those for which asymmetric drift or large random motions are relevant. In total we have compiled 2,780 measurements, of which 2,174, 506 and 100 are from gas kinematics, star kinematics and masers, respectively (see Supplementary Text). For each measurement, we translate the kinematic data into a constraint on the angular velocity  $\omega_c = v_c/R$  and on the Galactocentric radius  $R$ . The upper panel of Fig. 1 shows the rotation curve  $v_c(R)$  for the full compilation of data, including only statistical uncertainties (see Supplementary Text for a test of systematics on observational data).

The contribution of stars and gas to the total mass of the Galaxy has historically been subject to significant uncertainties, in particular towards the innermost regions where its dynamical role is most important. Substantial progress has been made recently, and data-based models that encode the three-dimensional morphology of the baryonic distribution have become available in the literature. To bracket the uncertainties on the stellar and gas distributions, we consider here all possible combinations of a set of detailed models for the stellar bulge<sup>14–19</sup>, stellar disk<sup>20–24</sup> and gas<sup>25,26</sup> (see Supplementary Text). The stellar bulge models encompass alternative density profiles in the inner few kiloparsecs and different configurations of the Galactic bar. The stellar disks implemented provide instead the best descriptions of star observations across the Galaxy, including parameterizations with and without separation into thin and thick populations. Finally, the gas is split into its molecular, atomic (cold, warm) and ionized (warm, hot, very hot) components, paying special attention to the localized features in the range  $R = 10\text{ pc} \text{--} 20\text{ kpc}$ .

The gravitational potential of each model is computed through multipole expansion<sup>32</sup>, and the corresponding rotation curve is shown in the lower panel of Fig. 1 with its original normalization. We calibrated each bulge with the microlensing optical depth measurement towards the central Galactic region<sup>33,34</sup>  $\langle \tau \rangle = 2.17^{+0.47}_{-0.38} \times 10^{-6}$ , each disk with the dynamical constraint

<sup>1</sup>Instituto de Física Teórica UAM/CSIC, C/ Nicolás Cabrera 13-15, 28049 Cantoblanco, Madrid, Spain. <sup>2</sup>ICTP South American Institute for Fundamental Research, and Instituto de Física Teórica—Universidade Estadual Paulista (UNESP), Rua Dr. Bento Teobaldo Ferraz 271, 01140-070 São Paulo, SP, Brazil.

<sup>3</sup>Physik-Department T30d, Technische Universität München, James-Frank-Straße, 85748 Garching, Germany. <sup>4</sup>The Oskar Klein Centre for Cosmoparticle Physics, Department of Physics, Stockholm University, AlbaNova, SE-106 91 Stockholm, Sweden. <sup>5</sup>GRAPPA Institute, University of Amsterdam, Science Park 904, 1090 GL Amsterdam, The Netherlands. \*e-mail: iocco@ift.unesp.br

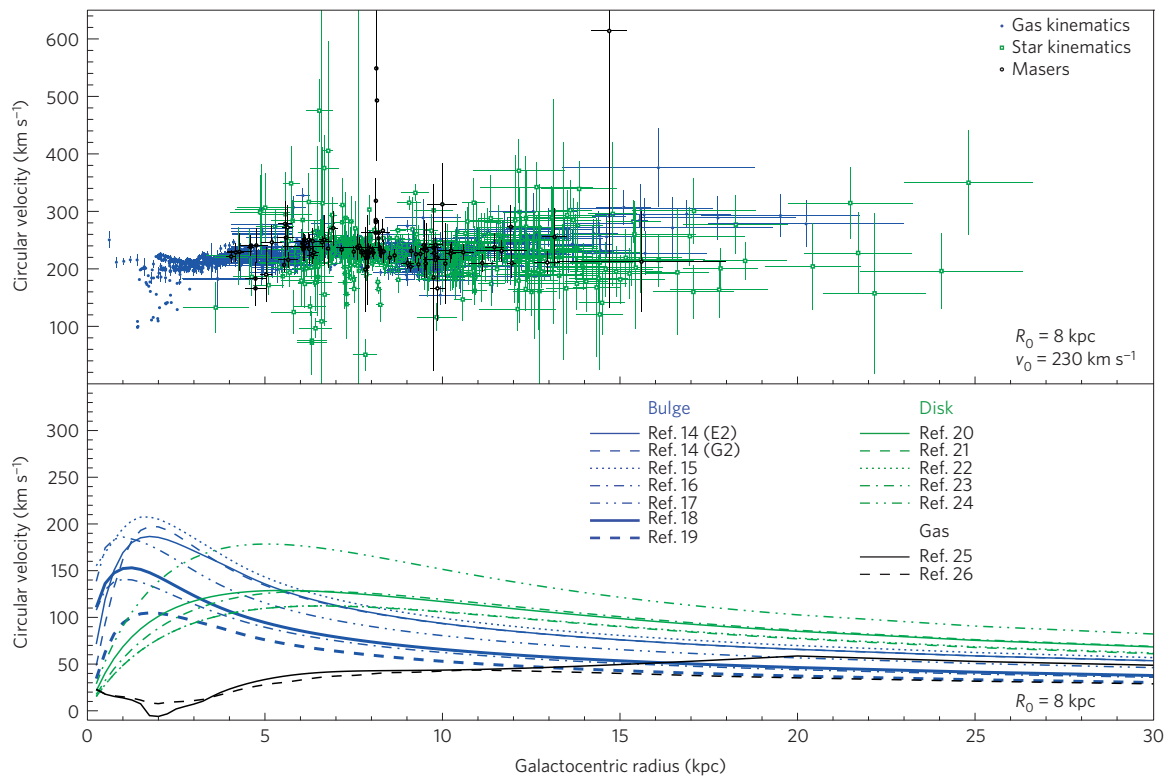


**Figure 1 | The rotation curve of the Milky Way.** In the top panel we show our compilation of rotation curve measurements as a function of Galactocentric radius, including data from gas kinematics (blue dots; HI terminal velocities, CO terminal velocities, HI thickness, HII regions, giant molecular clouds), star kinematics (open green squares; open clusters, planetary nebulae, classical cepheids, carbon stars) and masers (open black circles). Error bars correspond to  $1\sigma$  uncertainties. The bottom panel shows the contribution to the rotation curve as predicted from different models for the stellar bulge (blue), stellar disk (green) and gas (black). We assume a distance to the Galactic Centre  $R_0 = 8$  kpc in both panels, and a local circular velocity  $v_0 = 230$  km s $^{-1}$  in the top panel.

on the local total stellar surface density<sup>24</sup>  $\Sigma_* = 38 \pm 4 M_\odot \text{pc}^{-2}$ , and for the gas we adopted a CO-to-H<sub>2</sub> conversion factor of<sup>25,35</sup>  $(0.5 - 3.0) \times 10^{20} \text{cm}^{-2} (\text{K km s}^{-1})^{-1}$  for  $R > 2$  kpc. This procedure ensures that all baryonic models comply with the existing observational constraints and moreover it assigns a realistic uncertainty to the contribution of each model to the rotation curve. Note that we do not attempt to account for the poorly understood systematics of each single baryonic model, but instead use the spread due to all morphological configurations as an estimate of the systematics on the baryonic contribution.

We assess the evidence for an unseen (dark) component of the gravitational potential of our Galaxy in the form of a discrepancy between the observed rotation curve,  $\omega_c$ , and that expected from the set of baryonic models described above,  $\omega_b$ . We stress that we do not make any assumption about the nature or distribution of dark matter: our analysis therefore provides a model-independent estimate of the amount of dark matter in the Galaxy. For each baryonic model, the two-dimensional chi-square<sup>3</sup> is computed and used to assess the goodness-of-fit. We have explicitly checked through Monte Carlo calculations that this statistic has an approximate  $\chi^2$  distribution for the case at hand. The analysis is restricted to Galactocentric radii  $R > R_{\text{cut}} = 2.5$  kpc, below which the orbits of the kinematic tracers are significantly non-circular. We adopt a distance to the Galactic Centre  $R_0 = 8$  kpc, a local circular velocity  $v_0 = 230$  km s $^{-1}$ , and a peculiar solar motion<sup>36</sup>  $(U, V, W)_\odot = (11.10, 12.24, 7.25)$  km s $^{-1}$ .

The upper panel of Fig. 2 shows the angular velocity as a function of the Galactocentric radius. Observational data are shown with red dots, and the grey band shows the envelope of all baryonic models discussed above, which we interpret here as bracketing the possible

contribution of baryons to the rotation curve. The discrepancy between observations and the expected contribution from baryons is evident above Galactocentric radii of 6–7 kpc. The residuals  $(\omega_c^2 - \omega_b^2)^{1/2}$  are plotted in the middle panel of Fig. 2 for a fiducial baryonic model<sup>14,24,25</sup> (the one shown by the black solid line in the upper panel), and they can be readily interpreted as the contribution of an extra component to the Newtonian gravitational potential of our Galaxy. Interestingly, the gravitational potential from a dark matter distribution such as those suggested by numerical simulations (Navarro–Frenk–White or Einasto profiles) smoothly fills the gap without fine tuning. We stress that we do not perform a fit of the dark matter profile parameters to the data, but simply superimpose the residuals expected from a standard Navarro–Frenk–White profile as typically implemented in the literature.

The main conclusion of our analysis is summarized in the bottom panel of Fig. 2, where we plot the  $\chi^2$  per degree of freedom for each baryonic model and for all data up to a given radius  $R$  (but above  $R_{\text{cut}}$ ). The evidence for a dark component rises above  $5\sigma$  (thick red line) well inside the solar circle for all baryonic models. Indeed, whereas the relative discrepancy between observational data and baryonic models is higher at larger Galactocentric radii, it is at lower radii that uncertainties are smallest. Hence, the evidence grows swiftly at relatively small radii and saturates above  $R_0$ . We have tested the robustness of our results against variations of  $R_0$ ,  $v_0$ , peculiar solar motion and data selection as well as against systematics due to spiral arms<sup>7</sup>. The results change only mildly for all cases, and the conclusions drawn from Fig. 2 remain unchanged (see Supplementary Text).

The comparison of the Milky Way observed rotation curve with the predictions of a wide array of baryonic models points strongly

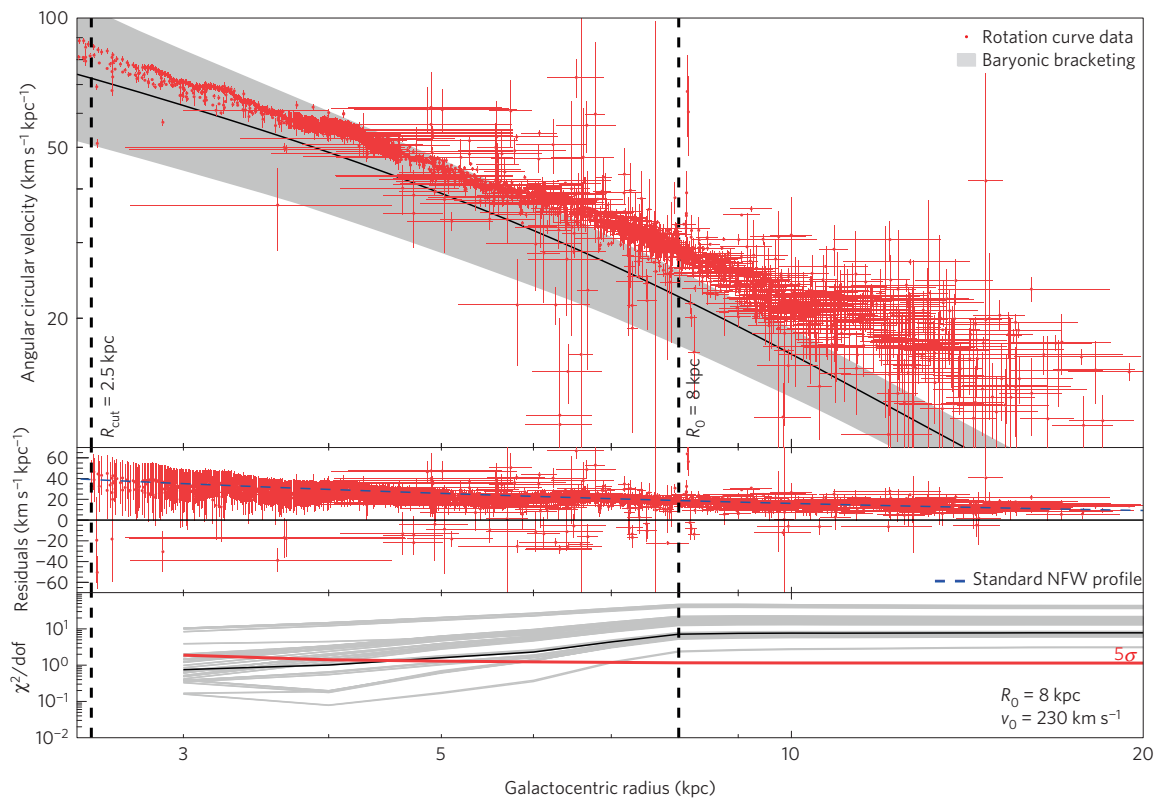


**Figure 2 | Evidence for dark matter.** In the top panel we show the angular velocity measurements from the compilation shown in Fig. 1 (red dots) together with the bracketing of the contribution of all baryonic models (grey band) as a function of Galactocentric radius. Error bars correspond to  $1\sigma$  uncertainties, and the grey band shows the envelope of all baryonic models including  $1\sigma$  uncertainties. The contribution of a fiducial baryonic model is marked with the black line. The residuals  $(\omega_c^2 - \omega_b^2)^{1/2}$  between observed and predicted angular velocities for this baryonic model are shown in the central panel. The blue dashed line shows the contribution of a Navarro-Frenk-White profile with scale radius of 20 kpc normalized to a local dark matter density of  $0.4 \text{ GeV cm}^{-3}$ . The bottom panel shows the cumulative reduced  $\chi^2$  for each baryonic model as a function of Galactocentric radius. The black line shows the case of the fiducial model plotted in black in the top panel, and the thick red line represents the reduced  $\chi^2$  corresponding to  $5\sigma$  significance. In this figure we assume a distance to the Galactic Centre  $R_0 = 8 \text{ kpc}$  and a local circular velocity  $v_0 = 230 \text{ km s}^{-1}$ , and we ignore all measurements below  $R_{\text{cut}} = 2.5 \text{ kpc}$ .

to the existence of a contribution to the gravitational potential of the Galaxy from an unseen, diffuse component. The statistical evidence is very strong already at small Galactocentric radii, and it is robust against uncertainties on Galactic morphology and kinematics. Without any assumption about the nature of this dark component of matter, our results open a new avenue for the determination of its distribution inside the Galaxy. This has powerful implications both on studies aimed at understanding the structure and evolution of the Milky Way in a cosmological context, and on direct and indirect dark matter searches, aimed at understanding the very nature of dark matter.

Received 10 June 2014; accepted 24 December 2014;  
published online 9 February 2015

## References

- Bertone, G. *Particle Dark Matter: Observations, Models and Searches* (Cambridge Univ. Press, 2010).
- Read, J. I. The local dark matter density. *J. Phys. G* **41**, 063101 (2014).
- Fich, M., Blitz, L. & Stark, A. A. The rotation curve of the Milky Way to  $2R(0)$ . *Astrophys. J.* **342**, 272–284 (1989).
- McClure-Griffiths, N. M. & Dickey, J. M. Milky Way kinematics. I. Measurements at the subcentral point of the fourth quadrant. *Astrophys. J.* **671**, 427–438 (2007).
- Luna, A., Bronfman, L., Carrasco, L. & May, J. Molecular gas, kinematics, and OB star formation in the spiral arms of the southern Milky Way. *Astrophys. J.* **641**, 938–948 (2006).
- Honma, M. & Sofue, Y. Rotation curve of the galaxy. *Publ. Astron. Soc. Jpn* **49**, 453–460 (1997).
- Brand, J. & Blitz, L. The velocity field of the outer galaxy. *Astron. Astrophys.* **275**, 67 (1993).
- Hou, L. G., Han, J. L. & Shi, W. B. The spiral structure of our Milky Way Galaxy. *Astron. Astrophys.* **499**, 473–482 (2009).
- Frinchaboy, P. M. & Majewski, S. R. Open clusters as galactic disk tracers. I. Project motivation, cluster membership, and bulk three-dimensional kinematics. *Astron. J.* **136**, 118–145 (2008).
- Durand, S., Acker, A. & Zijlstra, A. The kinematics of 867 galactic planetary nebulae. *Astron. Astrophys. Suppl.* **132**, 13–20 (1998).
- Pont, F., Queloz, D., Bratschi, P. & Mayor, M. Rotation of the outer disc from classical cepheids. *Astron. Astrophys.* **318**, 416–428 (1997).
- Battinelli, P., Demers, S., Rossi, C. & Gigoyan, K. S. Extension of the C star rotation curve of the Milky Way to 24 kpc. *Astrophysics* **56**, 68–75 (2013).
- Reid, M. J. *et al.* Trigonometric parallaxes of high mass star forming regions: The structure and kinematics of the Milky Way. *Astrophys. J.* **783**, 130 (2014).
- Stanek, K. Z. *et al.* Modeling the galactic bar using red clump giants. *Astrophys. J.* **477**, 163–175 (1997).
- Zhao, H. A steady-state dynamical model for the COBE-detected galactic bar. *Mon. Not. R. Astron. Soc.* **283**, 149–166 (1996).
- Bissantz, N. & Gerhard, O. Spiral arms, bar shape and bulge microlensing in the Milky Way. *Mon. Not. R. Astron. Soc.* **330**, 591–608 (2002).
- López-Corredoira, M. *et al.* The long bar in the Milky Way: Corroboration of an old hypothesis. *Astron. J.* **133**, 154–161 (2007).
- Vanhollebeke, E., Groenewegen, M. A. T. & Girardi, L. Stellar populations in the Galactic bulge. Modelling the Galactic bulge with TRILEGAL. *Astron. Astrophys.* **498**, 95–107 (2009).
- Robin, A. C., Marshall, D. J., Schultheis, M. & Reylé, C. Stellar populations in the Milky Way bulge region: Towards solving the Galactic bulge and bar shapes using 2MASS data. *Astron. Astrophys.* **538**, A106 (2012).
- Han, C. & Gould, A. Stellar Contribution to the Galactic Bulge Microlensing Optical Depth. *Astrophys. J.* **592**, 172–175 (2003).

21. Calchi Novati, S. & Mancini, L. Microlensing towards the large magellanic cloud: Self-lensing for OGLE-II and OGLE-III. *Mon. Not. R. Astron. Soc.* **416**, 1292–1301 (2011).
22. De Jong, J. T. A. *et al.* Mapping the stellar structure of the Milky Way thick disk and halo using SEGUE photometry. *Astrophys. J.* **714**, 663–674 (2010).
23. Jurić, M. *et al.* The Milky Way tomography with SDSS. I. Stellar number density distribution. *Astrophys. J.* **673**, 864–914 (2008).
24. Bovy, J. & Rix, H.-W. A direct dynamical measurement of the Milky Way's disk surface density profile, disk scale length, and dark matter profile at  $4 \text{ kpc} < R < 9 \text{ kpc}$ . *Astrophys. J.* **779**, 115 (2013).
25. Ferriere, K. Global model of the interstellar medium in our galaxy with new constraints on the hot gas component. *Astrophys. J.* **497**, 759–776 (1998).
26. Moskalenko, I. V., Strong, A. W., Ormes, J. F. & Potgieter, M. S. Secondary antiprotons and propagation of cosmic rays in the galaxy and heliosphere. *Astrophys. J.* **565**, 280–296 (2002).
27. Navarro, J. F., Frenk, C. S. & White, S. D. M. The structure of cold dark matter halos. *Astrophys. J.* **462**, 563 (1996).
28. Merritt, D., Graham, A. W., Moore, B., Diemand, J. & Terzić, B. Empirical models for dark matter halos. I. Nonparametric construction of density profiles and comparison with parametric models. *Astron. J.* **132**, 2685–2700 (2006).
29. Catena, R. & Ullio, P. A novel determination of the local dark matter density. *J. Cosmol. Astropart. Phys.* **8**, 4 (2010).
30. Sofue, Y., Honma, M. & Omodaka, T. Unified rotation curve of the galaxy – decomposition into de vaucouleurs bulge, disk, dark halo, and the 9-kpc rotation dip –. *Publ. Astron. Soc. Jpn* **61**, 227–236 (2009).
31. Bhattacharjee, P., Chaudhury, S. & Kundu, S. Rotation curve of the Milky Way out to  $\sim 200 \text{ kpc}$ . *Astrophys. J.* **785**, 63 (2014).
32. Binney, J. & Tremaine, S. *Galactic Dynamics: Second Edition* (Princeton Univ. Press, 2008).
33. Popowski, P. *et al.* Microlensing optical depth toward the galactic bulge using clump giants from the MACHO survey. *Astrophys. J.* **631**, 879–905 (2005).
34. Iocco, F., Pato, M., Bertone, G. & Jetzer, P. Dark matter distribution in the Milky Way: Microlensing and dynamical constraints. *J. Cosmol. Astropart. Phys.* **11**, 29 (2011).
35. Ackermann, M. *et al.* Fermi-LAT observations of the diffuse  $\gamma$ -ray emission: Implications for cosmic rays and the interstellar medium. *Astrophys. J.* **750**, 3 (2012).
36. Schönrich, R., Binney, J. & Dehnen, W. Local kinematics and the local standard of rest. *Mon. Not. R. Astron. Soc.* **403**, 1829–1833 (2010).

### Acknowledgements

We acknowledge fruitful conversations on gas with L. Tibaldo. The authors thank the Kavli Institute for Theoretical Physics at the University of California, Santa Barbara for hospitality during the programme Hunting for Dark Matter. F.I. thanks the K. M. Gesellschaft for logistic support during the very early stages of this work, and the Wenner-Gren Stiftelserna for stipend support at the Oskar Klein Centre in Stockholm. M.P. acknowledges the support from Wenner-Gren Stiftelserna in Stockholm. G.B. acknowledges the support of the European Research Council through the ERC Starting Grant WIMPs Kairos.

### Author contributions

The three authors have contributed equally to the intellectual content of the paper and the design of the analysis.

### Additional information

Supplementary information is available in the [online version of the paper](#). Reprints and permissions information is available online at [www.nature.com/reprints](http://www.nature.com/reprints). Correspondence and requests for materials should be addressed to F.I.

### Competing financial interests

The authors declare no competing financial interests.